

# $\pi$ Cholesky: Polynomial Interpolation of Multiple Cholesky Factors for Efficient Approximate Cross-Validation

Da Kuang  
Georgia Institute of Technology  
da.kuang@cc.gatech.edu

Raffay Hamid  
DigitalGlobe  
raffay@cc.gatech.edu

## ABSTRACT

Performing  $k$ -fold cross validation to avoid over-fitting is a standard procedure in statistical learning. For least squares problems, validating each fold requires solving a linear system of equations, for which using Newton’s method is a popular choice. An efficient way to perform Newton’s method is to find the Cholesky decomposition of the Hessian matrix followed by forward and back-substitution. In this work, we demonstrate that performing Cholesky factorization for a dense set of regularization parameter values can be the dominant cost in cross validation, and therefore a significant bottleneck in large-scale learning. To overcome this challenge, we propose an efficient way to densely interpolate Cholesky factors computed over a sparsely sampled set of the regularization parameter values. This enables us to optimally minimize the hold-out error while incurring only a fraction of the computational cost. Our key insight is that Cholesky factors for different regularization parameter values lie over smooth curves that can be approximated using polynomial functions. We present a framework to learn these multiple polynomial functions simultaneously, and propose solutions to several efficiency challenges in the implementation of our framework. We show results on multiple data sets to demonstrate that using the interpolated Cholesky factors as opposed to the exact ones results in a substantial speed-up in cross-validation with no noticeable increase in the hold-out error.

## 1. INTRODUCTION

Least-squares linear regression has maintained its significance as a useful model and a worthy opponent to the more sophisticated learning methods. This is mainly because:

- a**– Its closed form solution can be solved efficiently by exploiting the modern hardware architecture using high performance software, such as BLAS-3 matrix computations [13].
- b**– Recent advances in kernel methods [2] [37] [35] [27] [22] [34] provide an efficient way to project data into non-linear space,

Permission to make digital or hard copies of all or part of this work for personal or classroom use is granted without fee provided that copies are not made or distributed for profit or commercial advantage and that copies bear this notice and the full citation on the first page. To copy otherwise, to republish, to post on servers or to redistribute to lists, requires prior specific permission and/or a fee.

KDD ’14 New York, NY, USA

Copyright 20XX ACM X-XXXXX-XX-X/XX/XX ...\$15.00.

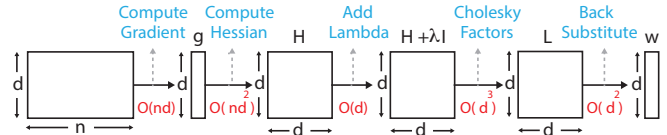


Figure 1: Computational pipeline of least squares regression along with the computational costs of the main steps.

where the closed form solution of linear regression can be used to efficiently learn non-linear models.

**c**– Availability of error correcting methods [10] [30] provides a way to increase the robustness of least squares to data outliers, and enable simultaneous learning of classifiers for multiple classes in a single pass over the data. This makes least squares particularly interesting for problems with a large number of classes and training points.

Like all statistical learning approaches however, least-squares regression also needs to resolve the central tradeoff between bias-versus-variance to generalize well over unseen data. A standard way to strike the right balance between this trade-off is to perform  $k$ -fold cross validation on the training data, and to pick a value for the regularization parameter  $\lambda$  that minimizes the expected value of the hold-out error [1].

An important aspect of cross validation is its computational cost particularly for large-scale problems. To put this cost in perspective, we show in Figure 1 the main steps required to solve a least squares problem using Newton’s method, and the corresponding costs associated with them. Note that this pipeline is equivalent to using the normal equation method to solve a least squares problem in numerical linear algebra [13].

For  $d$ -dimensional data, each fold of cross validation requires finding the optimal value of  $\lambda$  searched over a range of  $q$  values. This amounts to solving a linear system with  $d$  variables, represented by the  $d \times d$  Hessian matrix,  $q$  times for each of the  $k$  folds. Recall that solving this linear system using the Cholesky factorization of the Hessian costs  $\mathcal{O}(d^3)$  operations. The entire cost of  $k$ -fold cross validation therefore adds up to  $\mathcal{O}(kqd^3)$  operations. Other considerable costs in the least-squares pipeline include computing the Hessian which requires  $\mathcal{O}(nd^2)$  operations<sup>1</sup>. Comparing

<sup>1</sup>While each validation fold uses a different Hessian matrix, the overall cost for Hessian computation is still  $\mathcal{O}(nd^2)$ . This is because  $k$  different Hessian matrices for  $k$  subsets of the data can all be computed in a *single* pass over the data. Different  $k - 1$  sets of these  $k$  Hessian matrices can then be combined in  $\mathcal{O}((k - 1)d^2)$  operations to form the Hessian

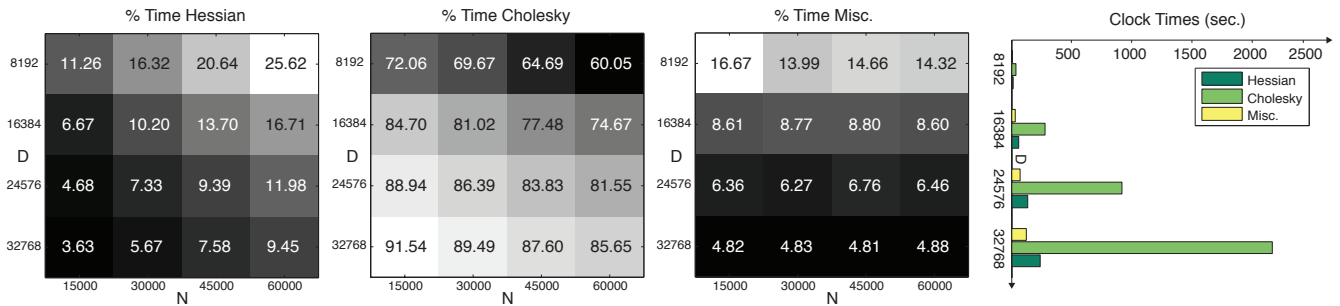


Figure 2: The figure shows the percentages of time taken by the three main steps in least-squares computational pipeline. Here we used MNIST [28] data projected using polynomial kernel [22] to different sized feature spaces. In Figures a, b, and c, the x-axis represents the number of training points, while the y-axis represents the size of the feature space. The plot for the miscellaneous times include gradient computation, forward- and back-substitution for solving a triangular system, and inexpensive operations such as memory allocation and copying *etc.* It can be seen that Cholesky factorization is by far the dominant computational cost for a large set of  $n$  and  $d$  combinations. Figure d shows the computational times taken to compute the Hessian, Cholesky factorization and to perform the various miscellaneous steps. We set the number of training instances to 60,000. Note that for larger  $d$ , Cholesky factorization is by far the dominant cost.

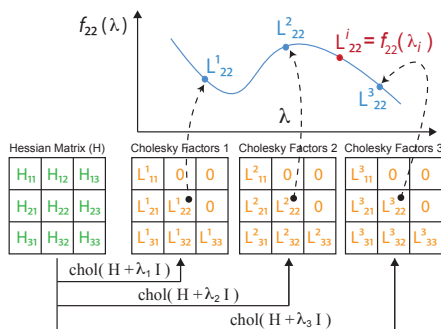


Figure 3: Illustrative figure showing the main idea behind the  $\pi$ Cholesky framework. Given a Hessian matrix  $H$ , we compute the Cholesky factors  $L^s$  of  $H + \lambda_s I$  for a small set  $\{\lambda_s\}$ . For all the  $(p, q)$ -th entries in these Cholesky factors ( $1 \leq p, q \leq d$ ), we fit a polynomial function  $f_{p,q}(\lambda)$ . These functions are used to efficiently estimate the entries of  $L$  for a larger set of  $\lambda$  values.

these costs, we conclude that for problems where  $n < kqd$ , the  $k$ -fold cross validation ends up being the overall dominant computational cost, especially for a large  $d$ . Figure 2 presents an empirical verification of the costs of cross validation versus Hessian as a function of  $n$  and  $d$ .

Our goal in this work is to reduce the overall computational cost of cross validation while incurring only a marginal increase in the expected hold-out error. The approach we take to achieve this goal is to densely interpolate the Cholesky factors of the Hessian matrix computed over a sparsely sampled set of  $\lambda$  values. The key observation that enables us to take this approach is that the Cholesky factors for different  $\lambda$  values tend to lie over smooth curves that can be approximated using polynomial functions (see Figure 3 for an illustration). We present an efficient way to learn these polynomial functions, and show that using these learned functions to search for the optimal value of  $\lambda$  results in a significant speed-up while not compromising the optimality of the  $\lambda$  selected by cross validation.

We formulate the problem of simultaneously learning these multiple smooth curves as a least squares problem with

matrix to be used in a particular validation fold. As  $n \gg (k-1)$ , the overall cost of Hessian computation is  $\mathcal{O}(nd^2)$ .

a shared Hessian and multiple gradients each corresponding to a particular entry in the lower-triangular Cholesky factor. This setup allows us to exploit the BLAS 3 [13] level matrix-matrix computations. Doing so however requires representing the lower-triangular part of the Cholesky factors in a vectorized form. This matrix to vector conversion if done naively can present a significant efficiency bottleneck. To solve this challenge, we propose a recursive strategy to access blocks of the lower-triangular Cholesky factor, and convert each block into a vector efficiently (see § 4.1 for more details). This novel block Cholesky vectorization strategy allows us to use the BLAS-3 based algorithm with only a nominal computational overhead.

Note that the accuracy of the fitted polynomial functions is in direct proportion to the number of exact Cholesky factors we use in the fitting procedure. However, to maximize the computational benefits of our approximation scheme, we need to minimize the number of exact Cholesky factorizations. To resolve this dilemma, we use a multi-level approach to quickly locate an appropriate interval first where candidate  $\lambda$  values are selected. This identification of the appropriate  $\lambda$  search range therefore increases both the robustness and overall efficiency of our framework.

To summarize, the **main contributions** of our work are:

- We propose the  $\pi$ Cholesky framework for densely interpolating Cholesky factors using multiple polynomial functions simultaneously computed over a sparsely sampled set of the regularization parameter. This enables us to optimally minimize the hold-out error in least squares problems with only a fraction of cost.
- We identify a set of important implementation challenges in the  $\pi$ Cholesky framework, and present novel solutions for them. Particularly noteworthy among these is a block Cholesky vectorization strategy that can be applied to any upper/lower-triangular matrix and is not only restricted to the scope of this work
- We present a comprehensive set of empirical analyses of the  $\pi$ Cholesky framework in comparison with several alternative approaches over multiple datasets.

In the following, we start by formalizing our problem and introducing the  $\pi$ Cholesky framework. We then highlight some of the critical implementational challenges in  $\pi$ Cholesky

framework and present our solutions for them. We then show timing and hold-out error results of our framework compared to alternative approaches on multiple datasets, and conclude by identifying future research directions.

## 2. RELATED WORK

Efficiently solving large sets of linear equations is critical for problems in a variety of research areas. Given the wide applicability of this topic, there has been substantial body of previous work on solving linear systems depending on their type [13] [6] [36] [9] and scale [23] [40]. As the matrix representation of linear systems makes them amenable to be solved computationally, a lot of the previous work on efficiently solving linear systems has particularly focused on matrix based methods [32]. In this paper, we consider the least squares problem that serves as the computational basis of linear regression. Popular amongst the methods to solve least squares problems are matrix decomposition methods such as Orthogonal-Triangular Decomposition (QR) [13], Cholesky<sup>2</sup> Factorization [19], and Singular Value Decomposition (SVD) [12]. Each of these methods pose different efficiency-stability trade-offs. However, for large dense least squares problems, Cholesky factorization has emerged as a method of choice which is used to solve the normal equation, *i.e.*, the linear system represented by the Hessian matrix of the least squares problem. This is mainly because of its storage advantages over QR and SVD (factor of 2 better) as well as its computational efficiency (factors of 2 and 39 better [13]). Due to these reasons, in this work we focus on Cholesky factorization to solve large, dense, and positive definite symmetric systems.

For many real-world problems however, a subset of the linear system parameters can undergo some change over a period of time. Solving such changing systems incrementally without having to recompute the entire solution every time a change occurs is therefore important from an efficiency viewpoint. A majority of the previous work in this context has mostly focused on rank-one or low-rank updates in the system parameters including direct matrix inverse [38] [16], LU decomposition [21] [20], Cholesky factorization [25], and Singular Value Decomposition [5] [15] [3].

Our problem setting is however different from such previous methods in two important ways: (i) as opposed to low-rank updates, we focus on linear systems undergoing a full rank update, and (ii) our updates are limited to the diagonal of the matrix representing the linear system. Both of these attributes are applicable to the problem of regularization for least-squares, as we will see in the next section.

The problem of efficient regularization for least squares has been previously explored in many different ways [41]. Arguably the most standard of these is to find the SVD of the input design matrix once, and then reuse the left and right singular vectors of the design matrix for different values of  $\lambda$ . While this method works well for relatively small problems, finding the SVD of a large design matrix even once can be prohibitively expensive. In such situations, truncated [18] or randomized approximate [17] SVD can be used. However their effectiveness for optimizing hold-out error in over-determined least squares problems is still unexplored (see § 5 for empirical evidence of this point).

<sup>2</sup>Recall that Lower-Upper (LU) [4] and Cholesky [19] factorizations are equivalent for symmetric metrics.

There has also been previous work to minimize the number of folds to validate during regularization [7] [8]. As our work focuses on reducing the amount of computational effort spent on exploring a set of  $\lambda$ 's in a given fold, it can be used in conjunction with such previous approaches [7] [8] to further improve the overall cross-validation performance.

## 3. *pi*CHOLESKY FRAMEWORK

### 3.1 Preliminaries

Let us define an  $n \times (d + 1)$  design matrix  $\mathbf{X}$  such that each row of  $\mathbf{X}$  holds one of the  $n$  training examples in a  $d$ -dimensional space appended by a scalar 1 to incorporate the intercept term. Similarly, let  $\mathbf{y}$  be the  $n$  dimensional vector containing all the target values of the training examples. Then the least squares cost function  $\mathbf{J}(\theta)$  can be defined as:

$$\mathbf{J}(\theta) = \frac{1}{2}(\mathbf{y} - \mathbf{X}\theta)^\top(\mathbf{y} - \mathbf{X}\theta) \quad (1)$$

Finding the derivative of  $\mathbf{J}(\theta)$  with respect to  $\theta$  gives:

$$\nabla_{\theta}\mathbf{J}(\theta) = \mathbf{X}^\top\mathbf{X}\theta - \mathbf{X}^\top\mathbf{y} \quad (2)$$

To minimize  $\mathbf{J}(\theta)$ , we set Equation 2 equal to zero, and obtain the normal equation:

$$\mathbf{X}^\top\mathbf{X}\theta = \mathbf{X}^\top\mathbf{y} \quad (3)$$

which results in the value of  $\theta$  that minimizes  $\mathbf{J}(\theta)$  as:

$$\theta = (\mathbf{X}^\top\mathbf{X})^{-1}\mathbf{X}^\top\mathbf{y} \quad (4)$$

In the context of Newton's method, we denote the Hessian matrix  $\mathbf{H}$  as  $\mathbf{X}^\top\mathbf{X}$  and the gradient vector  $\mathbf{g}$  as  $\mathbf{X}^\top\mathbf{y}$ . Hence Equation 4 can be re-written as:

$$\theta = \mathbf{H}^{-1}\mathbf{g} \quad (5)$$

While Equation 5 guarantees the minimization of the *bias* of our model to a given training set, it can run the risk of overfitting to its peculiarities, therefore resulting in high *variance* of the model. A standard way to strike the right balance between this bias-variance tradeoff in least squares problems is to use the Tychonov regularization [39] parameter  $\lambda$ , such that our regularized cost function becomes:

$$\mathbf{J}(\theta) = \frac{1}{2}(\mathbf{y} - \mathbf{X}\theta)^\top(\mathbf{y} - \mathbf{X}\theta) + \frac{\lambda}{2}\theta^\top\theta \quad (6)$$

Setting the derivative of  $\mathbf{J}(\theta)$  with respect to  $\theta$  equal to zero results in the following regularized solution of  $\theta$ :

$$\theta = (\mathbf{H} + \lambda\mathbf{I})^{-1}\mathbf{g} \quad (7)$$

where  $\mathbf{I}$  is the  $(d + 1) \times (d + 1)$  identity matrix. We can now attempt to settle the bias-variance tradeoff by solving Equation 7 for different values of  $\lambda$  in a  $k$ -fold cross-validation setting [24], and by picking the  $\lambda$  that in expectation gives the minimum hold-out error.

### 3.2 Least Squares using Cholesky Factors

Equation 7 can be rearranged as  $\mathbf{A}\theta = \mathbf{g}$ , where  $\mathbf{A}$  represents the regularized Hessian matrix  $\mathbf{H} + \lambda\mathbf{I}$ . For sufficiently

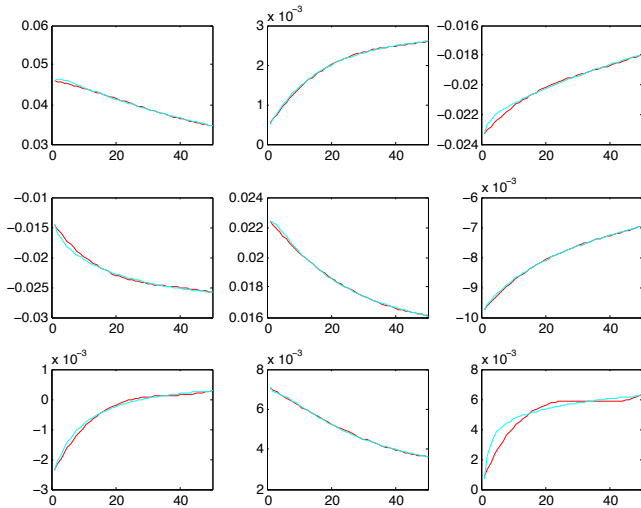


Figure 4: Each of these plots shows a particular entry in  $\mathbf{L}$  (y-axes) computed over different values of  $\lambda$  (x-axes) on the MNIST data [28]. The red curves show the entries in  $\mathbf{L}$  computed using exact Cholesky Factorization of  $\mathbf{A}$  for 50 values of  $\lambda$ , while the blue curves show the interpolated values of  $\mathbf{L}$  evaluated from  $3^{\text{rd}}$  order polynomial functions learned using 6 values of  $\lambda$ .

large values of  $\lambda$ ,  $\mathbf{A}$  is a full-rank symmetric positive definite matrix, and therefore we can apply Cholesky factorization  $\mathbf{A} = \mathbf{L}\mathbf{L}^T$ , where  $\mathbf{L}$  is a lower-triangular matrix. This enables us to re-write Equation 7 as:

$$\mathbf{L}\mathbf{L}^T\theta = \mathbf{g} \quad (8)$$

Representing  $\mathbf{L}^T\theta$  as  $\mathbf{w}$ , Equation 8 can be solved by a forward-substitution to solve the triangular system  $\mathbf{L}\mathbf{w} = \mathbf{g}$  for  $\mathbf{w}$  followed by a back-substitution to solve the triangular system  $\mathbf{L}^T\theta = \mathbf{w}$  for  $\theta$ . We can apply this procedure for multiple values of  $\lambda$  to find its optimal value that minimizes the expected hold-out error for each fold of cross-validation.

### 3.3 Cholesky Factors Interpolation

As we demonstrated in § 1 (Figure 2), solving Equation 7 using the Cholesky factorization of  $\mathbf{A} = \mathbf{H} + \lambda\mathbf{I}$  for multiple values of  $\lambda$  can be the dominant cost in the least-squares pipeline. To minimize this cost, we propose the *pi*Cholesky framework where we compute the Cholesky factors  $\mathbf{L}\mathbf{L}^T$  of  $\mathbf{A}$  over only a small set of  $\lambda$  values, followed by efficiently interpolating the corresponding entries in  $\mathbf{L}$  for a much more densely sampled set of  $\lambda$  values.

The key observation that makes this idea applicable is that corresponding entries of  $\mathbf{L}$  for different values of  $\lambda$  tend to lie over smooth curves that can be approximated using efficiently computable polynomial functions. Figure 4 illustrates this empirically, where the red curves show multiple corresponding entries in  $\mathbf{L}$  computed over different values of  $\lambda$  using exact Cholesky factorization for MNIST [28] data.

We now present the details of the *pi*Cholesky framework. Recall that for  $d$ -dimensional data, there are  $D = (d+1)(d+2)/2$  number of entries in the lower-triangular part of  $\mathbf{L}$ . Therefore, to interpolate a Cholesky factor based on those computed for different values of  $\lambda$ , we need to learn  $D$  polynomial functions, each corresponding to an entry in the lower-triangular part of  $\mathbf{L}$ .

---

#### Algorithm 1 – *pi*CHOLESKY

---

**Input:** Degree  $r$ , Set  $\{\lambda_s\}$  for  $s = \{1, 2, \dots, g\}$  and  $g > r$   
**Output:** A  $(r+1) \times D$  coefficient matrix  $\Theta$ , where  $D = (d+1)(d+2)/2$  and  $d$  is the dimensionality of training data

- 1: Find  $\mathbf{L}^s = \text{chol}(\mathbf{H} + \lambda_s\mathbf{I})$  for  $s = \{1, 2, \dots, g\}$
  - 2: Convert each  $\mathbf{L}^s$  into a row vector to construct the  $g \times D$  target matrix  $\mathbf{T}$
  - 3: Find the  $g \times g$  Vandermonde matrix  $\mathbf{W}$
  - 4: Extract the rightmost  $(r+1)$  columns of  $\mathbf{W}$  to form the  $g \times (r+1)$  observation matrix  $\mathbf{V}$
  - 5: Find  $\mathbf{G}_\lambda = \mathbf{V}^T\mathbf{T}$  and  $\mathbf{H}_\lambda = \mathbf{V}^T\mathbf{V}$
  - 6: Find  $\Theta = \mathbf{H}_\lambda^{-1}\mathbf{G}_\lambda$
- 

We pose the problem of efficient simultaneous learning of these polynomial functions as another least-squares problem. Recall that each polynomial function to be learned is of order  $r$ . We therefore need  $g > r$  exact Cholesky factors, each of which is computed using one of the  $g$  values of  $\lambda$ . Using these  $\lambda$  values, we compute the  $g \times g$  Vandermonde matrix  $\mathbf{W}$  [29]. We extract the rightmost  $(r+1)$  columns of  $\mathbf{W}$  to form our  $g \times (r+1)$  observation matrix  $\mathbf{V}$ . Our targets are the  $g$  rows of  $D$  values, where each row corresponds to the exact Cholesky matrix computed for one of the  $g$  values of  $\lambda$ . This forms our  $g \times D$  target matrix  $\mathbf{T}$ .

We can now define our least-squares cost function  $\mathbf{J}_\lambda(\Theta)$  as:

$$\mathbf{J}_\lambda(\Theta) = \frac{1}{2}(\mathbf{T} - \mathbf{V}\Theta)^T(\mathbf{T} - \mathbf{V}\Theta) \quad (9)$$

where  $\Theta$  is the  $(r+1) \times D$  polynomial coefficient matrix. Each column of  $\Theta$  represents the  $(r+1)$  coefficients of the  $D$  polynomial functions. Following similar procedure as described in § 3.1, the expression of  $\Theta$  can be written as

$$\Theta = \mathbf{H}_\lambda^{-1}\mathbf{G}_\lambda \quad (10)$$

Here  $\mathbf{H}_\lambda = \mathbf{V}^T\mathbf{V}$ , and  $\mathbf{G}_\lambda = \mathbf{V}^T\mathbf{T}$ .

Once we obtain all the polynomial coefficients  $\Theta$ , given a new regularization parameter value  $\lambda_t$ , the corresponding value of  $\mathbf{L}^t$  can be computed simply by evaluating the  $D$  polynomial functions at  $\lambda_t$ . The procedure for simultaneously learning the coefficients for the  $D$  polynomial functions is listed in Algorithm 1. The interpolation results using Algorithm 1 for the Cholesky factors computed on the MNIST data [28] are shown with blue curves in Figure 4. Here we set  $g = 5$  and  $r = 3$ . As can be seen from the figure, the blue plots (interpolated) trace the red plots (exact) quite closely.

**Computational Complexity:** We now discuss the theoretical computational complexity of Algorithm 1. We will turn to the practical computational challenges of Algorithm 1 in § 4. Note that the computationally dominant step of Algorithm 1 is evaluating  $\mathbf{L}^s$  for  $s = 1, 2, \dots, g$ , which requires  $\mathcal{O}(gd^3)$  operations. The only other noteworthy steps of Algorithm 1 are finding  $\mathbf{G}_\lambda$  and  $\Theta$  each of which takes  $\mathcal{O}(Dgr)$  operations<sup>3</sup>. Since  $d \gg r$ , the overall asymptotic cost of Algorithm 1 turns out to be  $\mathcal{O}(gd^3)$ . Furthermore, it only takes  $\mathcal{O}(Dr)$  operations to evaluate the interpolated Cholesky factor  $\mathbf{L}^t$  for each new value  $\lambda_t$ .

<sup>3</sup>Other steps of Algorithm 1 require finding  $\mathbf{H}_\lambda$  ( $\mathcal{O}(g^2r)$  operations), and inverting  $\mathbf{H}_\lambda$  ( $\mathcal{O}(r^3)$  operations), both of which are insignificant in comparison.

## 4. IMPLEMENTATIONAL CHALLENGES

### 4.1 Vectorizing a Cholesky Factor

So far we have assumed that the Cholesky factor computed for each  $\lambda$  in the sparsely sampled set of  $\lambda$  values is stored into a row vector represented by one row of the target matrix  $\mathbf{T}$  in Algorithm 1. Thus, efficient BLAS-3 level functions can be conveniently called when computing  $\mathbf{G} = \mathbf{V}^T \mathbf{T}$  and  $\Theta = \mathbf{H}_\lambda^{-1} \mathbf{G}_\lambda$ . However, in Algorithm 1 we did not account for the computational cost of transforming a Cholesky factor into a row vector, which can turn out to be non-trivial (see below and Table 1 for more information). We now present an efficient way to transform a Cholesky factor into a vector so that we can use BLAS-3 level functions on it.

Let us denote the submatrix of a matrix  $\mathbf{M}$  as  $\mathbf{M}(i : j, r : s)$ , where  $i : j$  indicates the row indices  $i, i + 1, \dots, j$  and  $r : s$  indicates the column indices  $r, r + 1, \dots, s$  of the submatrix. For the sake of simplicity, we use  $h = d + 1$  as the dimension of a Cholesky factor  $\mathbf{L}$ . As  $\mathbf{L}$  is lower-triangular, a naive way to transform it into a row vector is to concatenate its lower-triangular portion row by row, *i.e.*,

$$\mathbf{L}(1, 1), \mathbf{L}(2, 1 : 2), \dots, \mathbf{L}(i, 1 : i), \dots, \mathbf{L}(h, 1 : h) \quad (11)$$

We call the ordering of entries of  $\mathbf{L}$  in Equation 11 as the **row-wise** strategy. However, this concatenation incurs non-continuous memory copy and, as shown in column 2 of Table 1, costs a considerable amount of time.

An alternative way to transform a Cholesky factor into a vector is to simply vectorize the entire matrix, that is, both the lower-triangular part (including the diagonal) and the all-zero upper-triangular part, *i.e.*,

$$\mathbf{L}(1, 1 : h), \mathbf{L}(2, 1 : h), \dots, \mathbf{L}(i, 1 : h), \dots, \mathbf{L}(h, 1 : h) \quad (12)$$

We call the ordering of entries of  $\mathbf{L}$  in Equation 12 as the **full-matrix** strategy. This over-simplistic strategy requires little extra cost because the matrix  $\mathbf{L}$  is internally stored as a one-dimensional array, one row after another. However, the subsequent interpolation step (line 5-6 in Algorithm 1) requires twice the computational cost of the interpolation step following the row-wise strategy, because  $D = (d + 1)^2$  instead of  $(d + 1)(d + 2)/2$  when we vectorize the entire Cholesky factor. Thus, the full-matrix strategy incurs a waste of computation, that has an adverse effect on the efficiency (see column 3 of Table 1 for empirical details).

Due to the unsatisfactory performances of both the row-wise and full-matrix strategies, we design an efficient strategy to vectorize the lower-triangular part of a Cholesky factor. Our goal here is two-fold: (i) to achieve continuous memory copy and, (ii) to have non-redundant computation in the interpolation step. Without the loss of generality, let us assume  $h$  is a power of two. We use a divide-and-conquer strategy to partition the lower-triangular part into a square matrix and two smaller lower-triangular matrices, *i.e.*,

$$\begin{aligned} \mathbf{L}^{12} &= \mathbf{L}\left(\frac{h}{2} + 1 : h, 1 : \frac{h}{2}\right) \\ \mathbf{L}^{11} &= \mathbf{L}\left(1 : \frac{h}{2}, 1 : \frac{h}{2}\right) \\ \mathbf{L}^{22} &= \mathbf{L}\left(\frac{h}{2} + 1 : h, \frac{h}{2} + 1 : h\right) \end{aligned} \quad (13)$$

This strategy is depicted in Figure 5(a). The vectorization of  $\mathbf{L}$  is the concatenation of the vectorizations of  $\mathbf{L}^{12}$ ,  $\mathbf{L}^{11}$ , and  $\mathbf{L}^{22}$ . To vectorize the square matrix  $\mathbf{L}^{12}$ , we can simply use

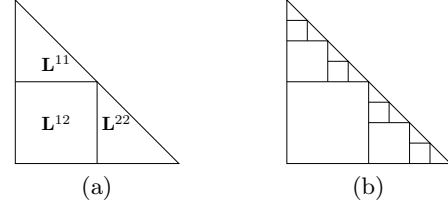


Figure 5: The **recursive** strategy to vectorize  $\mathbf{L}$ . (a) The partitioning of the lower-triangular part. (b) Final partitioning obtained by recursively applying the partitioning scheme in (a).

the ordering in the full-matrix strategy because  $\mathbf{L}^{12}$  has no special structure. For each of the smaller lower-triangular matrices  $\mathbf{L}^{11}$  and  $\mathbf{L}^{22}$ , we recursively partition its lower-triangular part using the partitioning scheme in Equation 13 until some threshold dimension  $h_0$  is reached. At the deepest level of the recursion, we use the row-wise strategy to vectorize the  $h_0 \times h_0$  matrix, which is not expensive for a sufficiently small  $h_0$ . The resulting recursive partitioning of the original Cholesky factor  $\mathbf{L}$  is depicted in Figure 5(b).

It is important to note that our proposed recursive vectorization strategy can be applied for the storage of any upper/lower-triangular matrix and is more generally applicable beyond the scope of this paper. Also note that for a system with column-major order for matrix storage rather than row-major order, vectorization in the row-wise and full-matrix strategies should be applied in a column-wise manner which results in a column vector instead of a row vector for efficiency reasons. Table 1 gives an empirical sense of the efficiency improvement brought about by our proposed recursive strategy compared to row-wise and full-matrix ones.

### 4.2 Choosing the Range of $\lambda$ Values

In Algorithm 1, the sparsely sampled set  $\{\lambda_s\}$  is chosen from an initial set of  $\lambda$  values. However, it remains to be determined how to select the initial set of  $\lambda$  values so that the optimal  $\lambda$  value that minimizes the hold-out error is included in that range. Now we propose a **multi-level** approach to select an appropriate range of  $\lambda$ . Intuitively, we start with a wide range and evaluate the hold-out errors for only a handful of  $\lambda$  values. After several iterations, we narrow ourselves to a small range for a finer search for the optimal  $\lambda$ .

More rigorously, let us assume that the candidate  $\lambda$  values are exponentially spaced and use the base 10 without the loss of generality. We define an initial range  $[10^{c-s}, 10^{c+s}]$  where  $c, s \in \mathbb{R}$  and  $s > 0$ . This initial range should be reasonably wide so that it includes any possible  $\lambda$  value in our consideration. At each iteration of the multi-level approach, we perform the following three steps:

1. Evaluate the hold-out errors  $h(\lambda)$  by computing the exact Cholesky factorization at a few exponentially spaced  $\lambda$  values in the current range.
2. Choose the  $\lambda$  value with the smallest hold-out error in Step 1, *i.e.*,  $\lambda_{\text{opt}} = \arg \min_{\lambda} h(\lambda)$ .
3. Update  $c, s$ :  $c \leftarrow \log \lambda_{\text{opt}}$ ,  $s \leftarrow s/2$ , and define the new range  $[10^{c-s}, 10^{c+s}]$ .

The procedure ends when  $s \leq s_0$  for a given value  $s_0 > 0$ .

**An Illustrative Example:** As an illustrative example, let us define  $c = -4, s = 5, s_0 = 1.5$  and the initial range to be equal to  $[10^{-9}, 10^{+1}]$  accordingly. We pick 3 values

Dimensions	Row-wise				Full-matrix				Recursive			
	Vec	Fit	Interp	Total	Vec	Fit	Interp	Total	Vec	Fit	Interp	Total
1024	1.48	0.33	1.25	<b>3.06</b>	0.15	0.72	2.47	<b>3.34</b>	0.79	0.33	1.27	<b>2.39</b>
2048	5.94	1.49	4.86	<b>12.29</b>	0.97	3.03	15.79	<b>19.79</b>	2.21	1.49	4.95	<b>8.65</b>
4096	29.85	5.79	27.46	<b>63.1</b>	3.76	11.46	59.9	<b>75.13</b>	6.66	5.85	27.64	<b>40.15</b>
8192	129.6	23.31	140.8	<b>293.7</b>	18.29	49.49	283.1	<b>350.9</b>	22.31	22.53	107.4	<b>152.3</b>
16384	500.9	98.83	515.76	<b>1116</b>	69.4	209.8	1041.8	<b>1321.1</b>	91.74	99.36	512.8	<b>703.9</b>

Table 1: Comparison of the timing results of  $\pi$ iCholesky before and after optimization, using MNIST data. The measured times (in seconds) include the transformation between an upper-triangular Cholesky factor and its vectorized form, as well as fitting and interpolating the polynomial functions, abbreviated as “vec”, “fit”, and “interp” respectively.

	Dimensionality	# Samples
<b>MNIST</b>	$28 \times 28$	60,000
<b>COIL-100</b>	$28 \times 28$	7,200
<b>Caltech-101</b>	$320 \times 200$	8,677
<b>Caltech-256</b>	$320 \times 200$	29,780

Table 2: A summary of the data sets we used in experiments.

$\lambda = 10^{c-s}, 10^c, 10^{c+s}$  in each iteration of the multi-level approach. After two iterations, we have  $s = 1.25 < s_0$  and we use the resulting range to build the sparsely sampled set  $\{\lambda_s\}$  as an input to Algorithm 1. We used the multi-level approach in our experiments with the parameters above, and for every data set we considered, this approach is able to find the appropriate  $\lambda$  range that includes the optimal  $\lambda$  value.

## 5. EXPERIMENTS

We now present the timing performances and approximation errors of our  $\pi$ iCholesky framework and compare it with standard and state-of-the-art methods. Our results show that the proposed method is able to accelerate large-scale linear regression substantially and achieve high accuracy in selecting the optimal regularization parameter.

### 5.1 Data Sets

We use four image data sets in our experiments. Some of the important details of these datasets are given below:

1. **MNIST** [28]: A widely-used data set of hand-written digits containing 60,000 examples in 784 dimensions.
2. **COIL-100** [33]: Images of 100 objects, each having 72 images with viewpoints equally spaced in the entire  $360^\circ$  range. The dimensionality of the data is 784.
3. **Caltech-101** [11]: Images of objects belonging to 101 categories with an average of 90 images per category. The size of each image is roughly  $300 \times 200$  pixels.
4. **Caltech-256**: Images of objects belonging to 256 categories with around 120 images per category. The size of each image is roughly  $300 \times 200$  pixels [14].

The size of images and number of examples in each data set is shown in Table 2. For MNIST and COIL-100, we projected the samples to 1023, 2047, 4095, 8191, and 16383 dimensions using the randomized polynomial kernel [22]. For the two Caltech data sets, we projected the samples to 16383 dimensions using the spatial pyramid framework [26]. All data-sets were converted to 2 class problems with equal numbers of positive and negative samples. In the following, we denote  $h = d + 1$  as the projected plus intercept dimensions.

### 5.2 Comparative Algorithms

We compare our  $\pi$ iCholesky framework with four alternative algorithms for solving least squares with cross validation:

1. **Exact Cholesky (Chol)** – Apply Cholesky factorization to the Hessian matrix  $\mathbf{H}$  for each candidate  $\lambda$  value as described in §3.2.
2. **Exact SVD (SVD)** – SVD is a standard method for solving ridge regression [31]. Given an  $n \times (d+1)$  design matrix  $\mathbf{X}$  and its SVD  $\mathbf{X} = \mathbf{U}\mathbf{\Sigma}\mathbf{V}^T$ , the solution of the coefficient vector  $\theta$  can be derived from Equation 7:
$$\theta = \mathbf{V} \text{diag} \left( \frac{\sigma_1}{\sigma_1^2 + \lambda}, \dots, \frac{\sigma_{d+1}}{\sigma_{d+1}^2 + \lambda} \right) \mathbf{U}^T \mathbf{g} \quad (14)$$
where  $\sigma_1, \dots, \sigma_{d+1}$  are the singular values of  $\mathbf{X}$  in non-increasing order.
3. **Truncated SVD (t-SVD)** – Instead of using the full SVD, we compute the  $k$  singular vectors  $\hat{\mathbf{U}}$  and  $\hat{\mathbf{V}}$  that correspond to the  $k$  largest singular values of  $\mathbf{X}$ , so that  $\mathbf{X}$  is approximated by  $\mathbf{X} \approx \hat{\mathbf{U}}\hat{\mathbf{\Sigma}}\hat{\mathbf{V}}^T$ , where  $\hat{\mathbf{U}} \in \mathbb{R}^{n \times k}$ ,  $\hat{\mathbf{\Sigma}} \in \mathbb{R}^{k \times k}$ ,  $\hat{\mathbf{V}} \in \mathbb{R}^{(d+1) \times k}$ . Then we obtain the coefficient vector  $\theta$  accordingly. We used an iterative solver to compute the truncated SVD which is faster than the algorithm for computing the full SVD.
4. **Randomized Approximate SVD (r-SVD)** – Random projections for matrix approximation can approximately solve the truncated SVD problem very efficiently. We use the algorithm described in [17].

The complexity of computing the exact SVD of  $\mathbf{X}$  is  $\mathcal{O}(2nd^2 + 11d^3)$  [13]. For  $n \leq d + 1$ , we compute the full SVD of the design matrix  $\mathbf{X}$  and the coefficient vector  $\theta$  as in Equation 14. For  $n > d$ , it is prohibitively more expensive to compute the full SVD for each fold of the training data than forming the Hessian first and computing its eigenvalue decomposition, though the latter is less numerically stable. Therefore, for the three SVD variations above, we use the Hessian-based framework described in §3.1 when  $n > d$  but replace Cholesky factorization with eigenvalue decomposition.

Recall that while QR decomposition is another feasible algorithm to solve the least squares problem [13], it is generally applied on the design matrix  $\mathbf{X}$ , and cannot be easily applied to linear regression with regularization. QR decomposition can also solve the linear system represented by the Hessian matrix directly as well, but it is more expensive than Cholesky factorization which exploits the symmetric and positive-definite property of the Hessian. Therefore, in our analysis we do not include the comparison with QR decomposition. Here we denote the  $\pi$ iCholesky framework as **PIChol**, and its multi-level version (§ 4.2) as **MPIChol**.

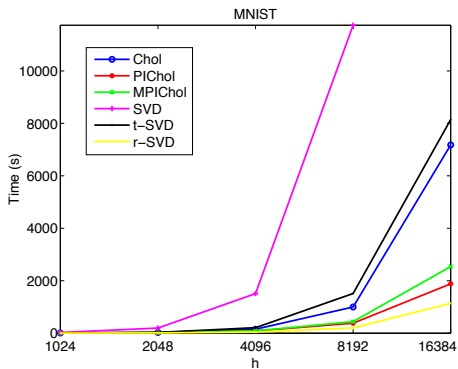


Figure 6: Times (in seconds) of the 6 considered algorithm as a function of  $h$  on MNIST data.

	MNIST	COIL -100	Caltech -101	Caltech -256
Chol	7178	6913	7055	6861
PIChol	1883	1669	1691	1735
MPIChol	2541	2350	2390	2381
SVD	94145	34889	90596	98232
t-SVD	8145	8583	10775	13181
r-SVD	1139	673	776	1114

Table 3: Time taken by the six algorithms when  $h = 16384$ . All times are reported in seconds.

### 5.3 Experiment Settings

For each data set, we search for the optimal  $\lambda$  value from a candidate set of 31 exponentially spaced  $\lambda$  values. For Chol, SVD, t-SVD, and r-SVD, the exact hold-out errors at those 31  $\lambda$  values are computed. For PIChol, we sparsely sample 4  $\lambda$  values from those 30 values and interpolate Cholesky factors using second-order polynomial functions, *i.e.*,  $g = 4$  and  $r = 2$  in Algorithm 1. The range from which candidate  $\lambda$  values are drawn is determined by the multi-level approach (§4.2). The ranges are set to  $[10^{-3}, 1]$ ,  $[10^{-3}, 1]$ ,  $[10^{-8}, 10^{-5}]$ , and  $[10^{-3}, 1]$  for the four data sets respectively.

For MPIChol, the range from which candidate  $\lambda$  values are drawn is adaptive, and we follow the experiment settings in §4.2. After the appropriate range is determined, we build a candidate set of 15 exponentially spaced  $\lambda$  values, and sparsely sample 3 values of  $\lambda$  from them to interpolate the Cholesky factors at the other  $\lambda$  value candidates.

### 5.4 Timing Results

Figure 6 and Table 3 show the timing results of the Cholesky and SVD-based algorithms. It can be observed that the PIChol and MPIChol methods have significant speedups over Chol. Moreover, the SVD and t-SVD are always the slowest. Finally, r-SVD is always the fastest algorithm; however, as we will see in the holdout-error results, r-SVD does not give any useful conclusions for the optimal  $\lambda$  value. Figure 6 shows the timings for the MNIST data. We obtained similar timing trends for all the four data-sets we used.

### 5.5 Hold-out Errors

Figure 7 shows the hold-out errors obtained for MNIST data when projected to 2048, 4096, 8192, and 16384 dimensions respectively. Similarly, Figure 8-a and b show the hold-

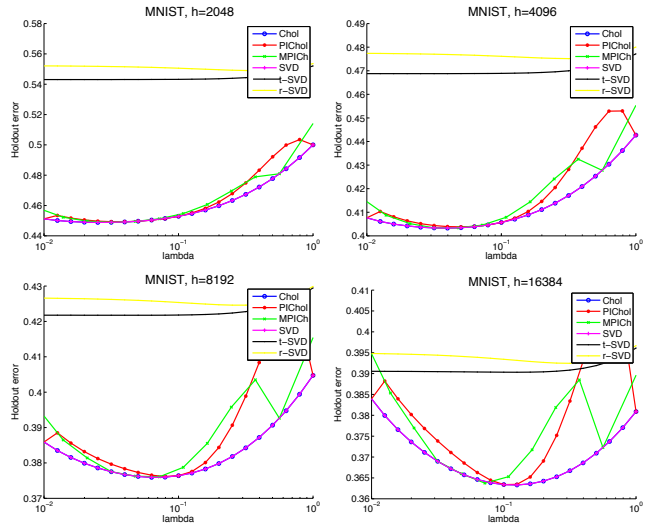


Figure 7: Hold-out errors for the six algorithms as a function of  $\lambda$  on the MNIST data.

out errors for COIL-100 data for 2048 and 4096 dimensions, while Figure 8-c and d show hold-out errors for Caltech 101 and Caltech 256 datasets for 16384 dimensions each. Table 4 shows the optimal hold-out error and the optimal  $\lambda$  value selected by each algorithm on the MNIST data set.

PIChol and MPIChol well approximate the performance of Chol. The approximation for  $h = 2048, 4096$  is better than that for  $h = 8192, 16384$ ; however, we notice that for the latter two cases with larger  $h$ , the approximation quality of PIChol and MPIChol is satisfactory when  $\lambda$  is close to the optimal  $\lambda$  value. This phenomenon justifies the effectiveness of our framework for choosing the optimal regularization parameter. From Table 4, we can compare PIChol and MPIChol more closely. We can see that the optimal  $\lambda$  value given by MPIChol is even closer to that given by Chol when  $h = 2048, 4096, 8192$ . When  $h = 16384$ , the optimal  $\lambda$  value given by MPIChol is a little farther away from that given by Chol, which can be explained by our sampling of 3  $\lambda$  values in the final range given by MPIChol for computing the exact Cholesky factorization, as opposed to the sampling of 4  $\lambda$  values for PIChol. Though t-SVD and r-SVD might be faster, they generate very poor approximation of the true hold-out error and the optimal  $\lambda$  value, and therefore its efficiency advantage is of little practical use.

Figure 9 shows the effectiveness of our multi-level approach for selecting the range of  $\lambda$  values in MPIChol for all the considered data sets. As an example for MNIST data, the algorithm first computes the hold-out error for  $\lambda = 10^{-9}, 10^{-4}, 10$  using exact Cholesky factorization and picked  $\lambda = 10$  as the one with the smallest error. It then computes the hold-out error for  $\lambda = 10^{-1.5}, 10, 10^{3.5}$  and picks  $\lambda = 10^{-1.5} \approx 0.0316$  as the one with the smallest error. Finally, it selects  $[10^{-2.75}, 10^{0.25}]$  as the range of candidate  $\lambda$  values, which is further explored in more detail using *pi*Cholesky framework. The candidate  $\lambda$  ranges for other data sets were similarly found, and are shown in Figure 9.

### 5.6 Normalized Root Mean Squared Error

Figure 10 shows the normalized root mean squared error (NRMSE) for least-squares polynomial fitting in PIChol on

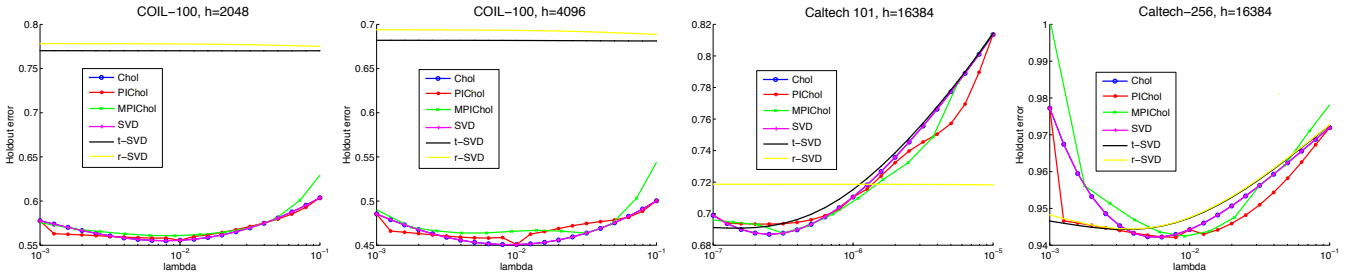


Figure 8: **a, b**– Hold-out errors for the six algorithms as a function of  $\lambda$  on the COIL-100 dataset for projection dimensions of 2048 and 4096 respectively. **c, d**– Hold-out errors for the six algorithms as a function of  $\lambda$  on Caltech 101 and Caltech 256.

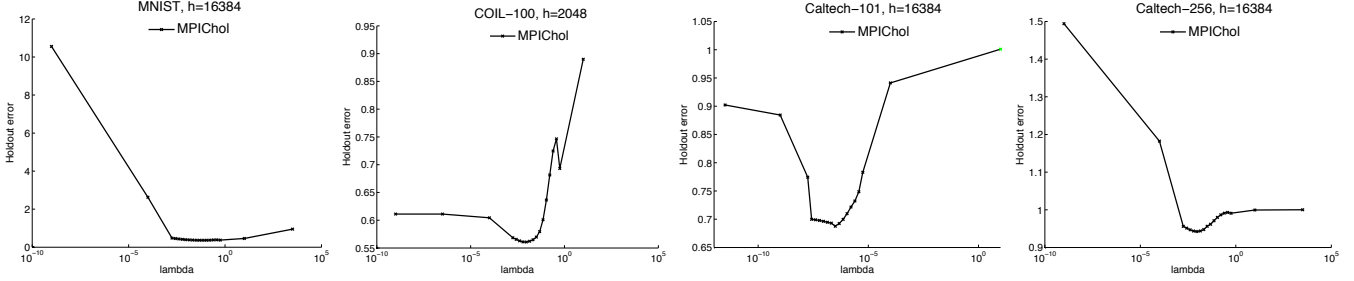


Figure 9: The hold-out error plot for `MPIChol` as a function of  $\lambda$  for MNIST, COIL-100, Caltech-101, and Caltech-256 datasets. The ranges are found by `MPIChol` for the four data-sets are  $[10^{-2.75}, 10^{-0.25}]$ ,  $[10^{-2.75}, 10^{-0.25}]$ ,  $[10^{-7.75}, 10^{-5.25}]$ , and  $[10^{-2.75}, 10^{-0.25}]$  respectively.

	$h = 2048$		$h = 4096$		$h = 8192$		$h = 16384$	
	Optimal hold-out error	Optimal $\lambda$						
<code>Chol</code>	0.4489	0.0251	0.4033	0.0398	0.3759	0.0631	0.3633	0.1259
<code>PIChol</code>	0.4493	0.0398	0.4038	0.0501	0.3762	0.0794	0.3634	0.1
<code>MPIChol</code>	0.4489	0.0316	0.4034	0.0316	0.3761	0.072	0.3637	0.072
<code>SVD</code>	0.4489	0.0251	0.4033	0.0398	0.3759	0.0631	0.3633	0.1259
<code>t-SVD</code>	0.5431	0.0063	0.4688	0.0126	0.4217	0.0398	0.3903	0.1259
<code>r-SVD</code>	0.5490	0.3981	0.4752	0.3162	0.4246	0.2512	0.3925	0.3162

Table 4: The optimal hold-out error and the optimal  $\lambda$  value selected by the six considered algorithms on MNIST data.

MNIST. Similar trends were found for the other considered data-sets. Recall that naively using the mean of target variable implies an NRMSE of 1. Our maximum NRMSE of 0.0457 therefore implies quite high interpolation accuracy.

## 6. CONCLUSIONS & FUTURE WORK

In this work, we showed that performing Cholesky factorization for dense sets of  $\lambda$  values can be the dominant cost in cross-validation, and therefore a significant bottleneck in large-scale learning. To overcome this challenge, we proposed an efficient way to densely interpolate Cholesky factors computed over a sparsely sampled set of  $\lambda$  values. This enabled us to exhaustively explore the space of  $\lambda$  values, and therefore optimally minimize the hold-out error while incurring only a fraction of the computational cost. The key insight that inspired our *pi*Cholesky framework was that Cholesky factors for different values of  $\lambda$  lie over smooth curves that can be approximated using polynomial functions. We presented a framework to learn these multiple polynomial functions simultaneously, and proposed solutions to several efficiency challenges in the implementation of our framework. Going forward, we plan to use the functions

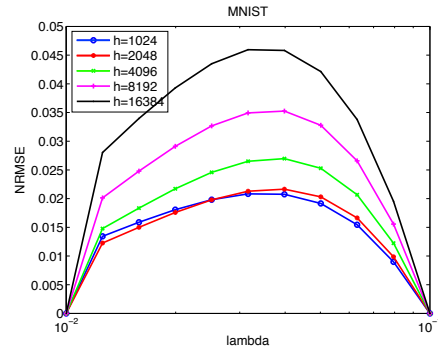


Figure 10: Normalized root mean square error (NRMSE) plot for *pi*Cholesky framework on MNIST data as a function of regularization parameter  $\lambda$ .

we learn in one fold to *warm-start* the learning process in a different fold. This strategy would reduce the number of exact Cholesky factorizations required in a fold, and would therefore further improve the performance of our framework.

## 7. REFERENCES

- [1] E. Alpaydin. *Introduction to machine learning*. MIT press, 2004.
- [2] L. Bottou, O. Chapelle, D. DeCoste, and J. Weston, editors. *Large-Scale Kernel Machines*. MIT Press, 2007.
- [3] M. Brand. Incremental singular value decomposition of uncertain data with missing values. In *Computer Vision & ECCV 2002*, pages 707–720. Springer, 2002.
- [4] J. R. Bunch and J. E. Hopcroft. Triangular factorization and inversion by fast matrix multiplication. *Mathematics of Computation*, 28(125):231–236, 1974.
- [5] J. R. Bunch and C. P. Nielsen. Updating the singular value decomposition. *Numerische Mathematik*, 31(2):111–129, 1978.
- [6] C. Cao, J. Dongarra, P. Du, M. Gates, P. Luszczek, and S. Tomov. cmlagma: High performance dense linear algebra with opencl.
- [7] G. C. Cawley and N. L. Talbot. Efficient leave-one-out cross-validation of kernel fisher discriminant classifiers. *Pattern Recognition*, 36(11):2585–2592, 2003.
- [8] G. C. Cawley and N. L. Talbot. Fast exact leave-one-out cross-validation of sparse least-squares support vector machines. *Neural networks*, 17(10):1467–1475, 2004.
- [9] T. A. Davis. *Direct methods for sparse linear systems*. Siam, 2006.
- [10] T. G. Dietterich and G. Bakiri. Solving multiclass learning problems via error-correcting output codes. *arXiv preprint cs/9501101*, 1995.
- [11] L. Fei-Fei, R. Fergus, and P. Perona. Learning generative visual models from few training examples: An incremental bayesian approach tested on 101 object categories. *CVIU*, 2007.
- [12] G. Golub and W. Kahan. Calculating the singular values and pseudo-inverse of a matrix. *Journal of the Society for Industrial & Applied Mathematics, Series B: Numerical Analysis*, 2(2):205–224, 1965.
- [13] G. H. Golub and C. F. Van Loan. *Matrix computations*. Johns Hopkins University Press, 2012.
- [14] G. Griffin, A. Holub, and P. Perona. Caltech-256 object category dataset. 2007.
- [15] M. Gu and S. C. Eisenstat. Dnating the singular value decomposition. *SIAM Journal on Matrix Analysis and Applications*, 16(3):793–810, 1995.
- [16] W. W. Hager. Updating the inverse of a matrix. *SIAM review*, 31(2):221–239, 1989.
- [17] N. Halko, P.-G. Martinsson, and J. A. Tropp. Finding structure with randomness: Probabilistic algorithms for constructing approximate matrix decompositions. *SIAM review*, 53(2):217–288, 2011.
- [18] P. C. Hansen. The truncatedsvd as a method for regularization. *BIT Numerical Mathematics*, 27(4):534–553, 1987.
- [19] R. A. Horn and C. R. Johnson. *Matrix analysis*. Cambridge university press, 2012.
- [20] M. Kaess, H. Johannsson, R. Roberts, V. Ila, J. Leonard, and F. Dellaert. isam2: Incremental smoothing and mapping with fluid relinearization and incremental variable reordering. In *Robotics and Automation (ICRA), 2011 IEEE International Conference on*, pages 3281–3288. IEEE, 2011.
- [21] M. Kaess, A. Ranganathan, and F. Dellaert. isam: Incremental smoothing and mapping. *Robotics, IEEE Transactions on*, 24(6):1365–1378, 2008.
- [22] P. Kar and H. Karnick. Random feature maps for dot product kernels. *Journal of Machine Learning Research*, 22:583–591, 2012.
- [23] S.-J. Kim, K. Koh, M. Lustig, S. Boyd, and D. Gorinevsky. An interior-point method for large-scale l1regularized least squares. *STSP*, 2007.
- [24] R. Kohavi et al. A study of cross-validation and bootstrap for accuracy estimation and model selection. In *IJCAI*, volume 14, pages 1137–1145, 1995.
- [25] I. Koutis, G. L. Miller, and R. Peng. A fast solver for a class of linear systems. *Communications of the ACM*, 55(10):99–107, 2012.
- [26] S. Lazebnik, C. Schmid, and J. Ponce. Beyond bags of features: Spatial pyramid matching for recognizing natural scene categories. In *CVPR*, 2006.
- [27] Q. Le, T. Sarlos, and A. Smola. Fastfood-computing hilbert space expansions in loglinear time. In *ICML*, pages 244–252, 2013.
- [28] Y. LeCun and C. Cortes. The mnist database of handwritten digits, 1998.
- [29] N. Macon and A. Spitzbart. Inverses of vandermonde matrices. *The American Mathematical Monthly*, 65(2):95–100, 1958.
- [30] F. MacWilliams and N. Sloane. The theory of error-correcting codes. 2006.
- [31] J. Mandel. Use of the singular value decomposition in regression analysis. *The American Statistician*, 36(1):15–24, 1982.
- [32] C. Meyer. *Matrix analysis and applied linear algebra book and solutions manual*, volume 2. Siam, 2000.
- [33] S. A. Nene, S. K. Nayar, and H. Murase. Columbia object image library (coil-100). Technical Report CUCS-006-96, Columbia University, 1996.
- [34] N. Pham and R. Pagh. Fast and Scalable Polynomial Kernels via Explicit Feature Maps. In *Proceedings of the 19th International Conference on Knowledge Discovery and Data Mining*, 2013.
- [35] A. Rahimi and B. Recht. Random features for large-scale kernel machines. *Advances in neural information processing systems*, 20:1177–1184, 2007.
- [36] Y. Saad. *Iterative methods for sparse linear systems*. Siam, 2003.
- [37] B. Scholkopf, C. J. C. Burges, and A. J. Smola, editors. *Advances in Kernel Methods: Support Vector Learning*. MIT Press, 1999.
- [38] J. Sherman and W. J. Morrison. Adjustment of an inverse matrix corresponding to a change in one element of a given matrix. *The Annals of Mathematical Statistics*, 21(1):124–127, 1950.
- [39] A. N. Tikhonov. On the stability of inverse problems. In *Dokl. Akad. Nauk SSSR*, volume 39, 1943.
- [40] H. A. Van der Vorst. *Iterative Krylov methods for large linear systems*, volume 13. Cambridge University Press, 2003.
- [41] C. R. Vogel. *Computational methods for inverse problems*, volume 10. Siam, 2002.